Structure of a-$GeSe_2$ from x-ray scattering measurements

P. H. Fuoss
AT&T Bell Laboratories, Holmdel, New Jersey 07733

A. Fischer-Colbrie*
Department of Materials Science and Engineering, Stanford University, Stanford, California 94305
(Received 15 September 1987)

Grazing-incidence x-ray scattering techniques have been used to study very thin (≥ 250 Å) films of amorphous $GeSe_2$. We find that the first sharp diffraction peak in these glasses arises from intrinsic features of chemically ordered tetrahedral bonding and not necessarily from a layered nature of the glass. We find no evidence of an oriented or layered structure and conclude that, if a layered structure is present, it must differ significantly from the crystalline phase.

I. INTRODUCTION

Determination of the structure of amorphous materials is a particularly complex problem. Currently, determination of the short-range order (e.g., first-neighbor bond lengths and coordination numbers) is fairly routine. However, most theories of amorphous structure predict a short-range environment similar to crystalline phases of the same composition and that significant deviations occur on length scales of 10 Å and longer. Correlations on these longer length scales have proven very difficult to characterize.

We report here x-ray scattering studies of amorphous (a-) $GeSe_2$ for films ranging from 250 Å to bulk thickness and discuss their structural implications. This paper includes the development and first application of the grazing-incidence x-ray scattering (GIXS) technique to study the structure of very thin amorphous layers on substrates. With GIXS it is possible to obtain the same information about the local and longer-range correlations in films as is obtained in x-ray studies of bulk amorphous materials.

These methods have been applied to evaporated and sputtered films of a-$GeSe_2$ in order to determine the structure and orientational dependence in the structure as a function of film thickness. Currently, there is considerable uncertainty about whether this material has intermediate-range order in the form of layers, or whether it is a chemically ordered random network with three-dimensional connectivity. These particular models generate scattering which will appear significantly different if layers are predominantly oriented by interaction with the substrate. Hence, by studying the evolution of the scattering from two-dimensional systems (thicknesses approximately the postulated size of the rafts) to three-dimensional systems, information about long-range correlations can be deduced.

In particular, we attempt to determine evidence of layers or any nonspherical (possibly cylindrical) aspects of the a-$GeSe_2$ structure with different film thicknesses and preparation techniques. This paper (1) describes the structural question and models of a-$GeSe_2$, (2) describes the GIXS experimental technique and results, (3) compares data to quasicrystalline (QC) models, including both spherical and cylindrical averages, and (4) presents a structural interpretation of these measurements.

II. MODELS

The two models which have been proposed for a-$GeSe_2$ have very similar features in the local order but differ in the intermediate-range order as well as the nature of like-atom bonds and phase separation. The first model is the chemically ordered covalent random-network (CRN) model, which consists of randomly bonded $GeSe_{4/2}$ tetrahedra linked to form a three-dimensional network.[1] In this model, the presence of like-atom bonds (Ge—Ge and Se—Se) or phase separation is attributed to defects.

In the second model, the raft model, proposed by Phillips,[2] the network is also presumed to consist predominantly of $GeSe_{4/2}$ tetrahedra, but these units are covalently bonded together in layers similar to those of crystalline $GeSe_2$. Each layer consists of parallel chains of corner-sharing tetrahedra, cross linked with pairs of edge-sharing tetrahedra. In the raft model, layers are terminated by Se-Se dimers parallel to the chains. Later Mössbauer work by Boolchand, Grothaus, Bresser, and Suranyi[3] suggests that the signal attributed to Se—Se bonds is more consistent with a raft which is six (50–60 Å) rather than two chains in width. In addition, results from Raman[4] spectroscopy as well as pressure and optical measurements[5] and laser recrystallization studies[6] of a-$GeSe_2$ have been used to support and extend Phillips's layer model.

In Phillips's model of a-$GeSe_2$, as in the crystal, the layers are held together by van der Waals forces. From neutron diffraction work,[7] Phillips suggests that correlations between layers are the origin of the first sharp diffraction peak (FSDP) in a-$GeSe_2$ and that the position and width of the peak are the result of an ~ 6-Å interlayer spacing with 60-Å correlation lengths (~ 10 layers). However, FSDP's are a common feature of chemically ordered tetrahedrally bonded liquids[8] and such an interpretation is not definitive.

 ©1988 The American Physical Society

III. EXPERIMENT

The GIXS geometry developed by Marra, Fuoss, and Eisenberger[9] is shown in Fig. 1. For our scattering measurements, the incident and scattered beams are fixed at small angles (ϕ and ϕ') with respect to the sample surface, while the sample and detector are scanned about the axis of the sample normal (θ-2θ). In this geometry, the scattering vector $k = 4\pi \sin(\theta)/\lambda$, is nearly parallel to the surface.

In addition to orienting k parallel to the sample surface, the surface sensitivity is greatly enhanced by using ϕ's near or below the angle for total external reflection. (Since the refractive index for x rays is slightly less than 1, Fresnel theory predicts that x rays will be totally reflected from the surface for grazing angles of order 0.1°.) Implications of this theory are the following. First, the penetration depth (normal to the sample) can be varied continuously from tens of Å to tens of micrometers by adjusting the incident angle, although at some angles, very small adjustments produce large changes in penetration depth. A minimum penetration depth of ~25 Å is obtained below the critical angle (~0.2° for 11-keV x rays) for total external reflection. In addition, at the critical angle there is an enhancement of the electric field (and therefore of the scattered intensity) at the surface of the sample. Slightly above the critical angle the signal does not fluctuate rapidly with very small changes in incident angle and the signal is near maximum. The measurements discussed here were performed in that region. For very thin samples there is the possibility of substrate contributions which can be minimized by using shallower grazing angles.

In quantitative analysis of the GIXS data, the structure-dependent scattering, normalized to a per-atom scattering strength, is obtained using methods similar to those described by Fuoss[10] with modifications related to the GIXS geometry. In particular, corrections are necessary for the angular (k) dependence of the polarization, $P(k)$, and for a detector function (or area correction), $D(k)$, related to the amount of illuminated sample seen by the detector. In these experiments, it is also necessary to account for a sample of finite thickness and substrate contributions, with appropriate absorption corrections for film, A_f, and substrate, A_s, terms. The measured signal I_m scaled by the normalization coefficient K is a function of the contributions from the film, I_f, substrate, I_s, and a k-independent background signal I_b due to either parasitic scattering or a fluorescence contribution:

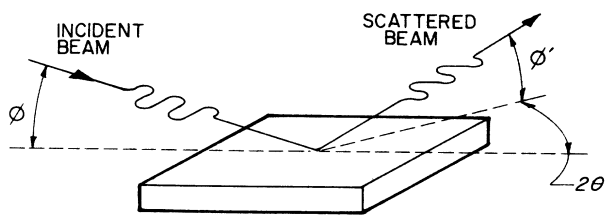

FIG. 1. The grazing-incident x-ray scattering geometry. X rays strike the sample at a grazing angle ϕ and the scattered x rays are detected at a combination of ϕ' and 2θ.

$$KI_m(k) = [I_f(k)A_fP(k) + I_s(k)A_sP(k) + I_b]D(k) . \quad (1)$$

K and I_b are constants in the above expression and are determined by the normalization procedure. After isolating $I_s(k)$, standard analysis techniques may be used [e.g., radial distribution function (RDF) analysis]. In this experiment, we have simplified the analysis by assuming that the crystalline substrate's only contribution to the measured intensity is Compton scattering. That is, we assume that Bragg-scattering and thermal diffuse scattering (TDS) intensities from the substrate are negligible since we were able to rotate the substrate to avoid those peaks.

Differential anomalous x-ray scattering (DAS) measurements were also performed on these samples. In the case of the films, Ge K-absorption-edge DAS measurements (11 000–11 090 eV) were performed. A complete set of Se K-absorption-edge (12 550–12 650 eV) data were not obtained due to beam time constraints. However, a preliminary data set was obtained for sputtered a-$GeSe_2$ films, and trends in these data will be discussed.

IV. RESULTS

Figure 2 shows the normalized scattered intensity for samples prepared by evaporation (250 Å, 1500 Å thick), sputtering (1500 Å), and quenching from the melt (bulk). The films were measured in the GIXS geometry, while the bulk sample was measured in the "conventional" symmetric Bragg (SB) geometry. The GIXS results were obtained with a focused wiggler (18 kG, 8 poles) beam line at the Stanford Synchrotron Radiation Lab (SSRL BL 4-2 end station) and typical peak count rates for the films were approximately 1 count/s per Å thickness with an incident-beam collimation of ~1.0 mrad. The bulk

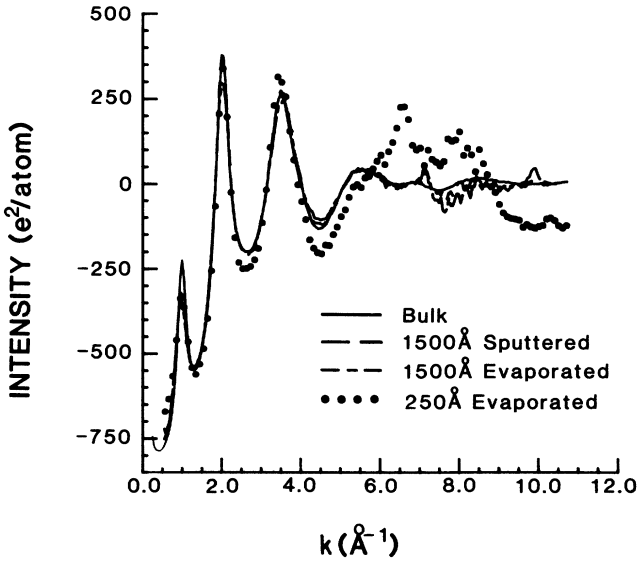

FIG. 2. The corrected, normalized scattered intensity from amorphous $GeSe_2$ as a function of thickness and sample preparation. The solid curve is data taken on a melt quenched bulk sample; the dashed curve is data from a 1500-Å-thick sputtered sample; the dotted-dashed curve is data from a 1500-Å-thick evaporated thick sample; the dotted curve is data from a 250-Å-thick evaporated sample.

sample was measured on an unfocused wiggler beam line (SSRL BL 4-3 side station) and count rates in the peaks were $\sim 10\,000$ counts/s for a 0.5-mrad beam.

The important differences between film and bulk curves are the small variations in peak height. These differences are sensitive to normalization parameters as well as to the experimental angular resolution. The large difference between the curve of the 250-Å-thick sample and those from the other samples is the peak at ~ 6.6 Å^{-1}, which is due to thermal diffuse scattering (TDS) from the (440) reflection of the Si substrate. (Other peaks can be observed for other azimuthal orientations of the substrate.) It is clear from these results that factors such as substrate contribution and polarization corrections become more important as the sample gets thinner, but the quality of the data in the lower angular range ($< k \sim 6$ Å) is reasonably good.

The apparent similarity between the film and the bulk material suggests that the film structure is spherically symmetric, since the bulk result is necessarily spherically symmetric (measurement of a powdered glass). We would intuitively expect that as the films become thinner, there would be a tendency for the layers to be oriented parallel to the surface. The GIXS geometry, which has its scattering vector parallel to the surface, would show a different scattering pattern for a cylindrically symmetric $GeSe_2$ film with its unique axis normal to the surface. Whether or not there are layers present in the material, the preceding result suggests that there is no evidence of such orientation in the film, down to 250 Å.

DAS data were obtained for both the 1500-Å-thick evaporated film and the melt-quenched bulk sample. The measurements of the scattering near the Ge and Se K absorption edges for the 1500-Å-thick film show that the bulk and film results are qualitatively similar. Unfortunately, difficulties in normalizing the data preclude an extensive analysis of the DAS results for the 1500-Å-thick films. However, for the bulk sample our results are totally consistent with the results of Fuoss, Eisenberger, Warburton, and Bienenstock.[11] Those are (1) the peak at 2 Å^{-1} almost totally disappears in the Ge-edge differential structure factor (DSF), implying that Se-Se correlations dominate that peak (i.e., the Ge-Ge and Ge-Se correlations cancel), and (2) the 1-Å^{-1} peak almost totally disappears in the Se DSF edge, implying that the 1-Å^{-1} peak is due to Ge-Ge correlations.

V. MODELING OF THE $GeSe_2$ STRUCTURE

In order to understand these results in more detail, we undertook an extensive modeling study of the structure of $GeSe_2$. We considered two types of models. The first was a spherical quasicrystalline (SQC) model following an algorithm developed by Taylor.[12] In the SQC model, a radial (spherical) distribution is created from all atomic correlations in the crystal, within a radius corresponding to the microcrystallite size. To simulate the structural disorder in an amorphous material, this distribution is broadened by a set of Gaussian functions which are centered on the peaks and have widths which increase with increasing interatomic distance. The scattering pattern is calculated from a Fourier transform of this distribution. The modeling parameters are the microcrystallite size and the dependence of the Gaussian widths on interatomic distance.

In the second model, the cylindrically symmetric quasicrystalline (CQC) model, an analogous approach is used. In this case, we create a cylindrical distribution (which is then broadened) from correlations which are in the plane parallel to the crystalline layers. The scattering pattern is calculated assuming that the momentum transfer is in the plane parallel to the layers as well as the sample surface. In this way, the layers are kept parallel to the surface but are rotationally random about the surface normal. The microcrystallite size input to the modeling calculation has three parameters in this case: (1) the lateral dimension parallel to the chains, (2) the number of chains included, and (3) the number of correlated layers. For these calculations, we used models which had only uncorrelated layers and models which had two layers which were correlated in the same manner as the crystalline phase.

The results of the modeling calculations which were optimized for a best fit to the data are shown in Figs. 3 and 4. As can be readily seen, the CQC model does not fit the data. In particular, the relative intensities of the peaks at ~ 2 and 3.5 Å^{-1} are reversed and the locations of 1- and 2-Å^{-1} peaks are incorrect. However, a low-k peak is produced, in spite of the fact that only correlations parallel to the layers are considered and interlayer correlations are not. We should emphasize that these calculations were optimized to fit the data. A more literal interpretation of the "raft" model produced fits which were much poorer.

On the other hand, the SQC model fits the data reasonably well, yielding good agreement on the 2- and 3.5-Å^{-1} peaks, but producing a 1-Å^{-1} peak which is too strong. This pattern corresponds to a microcrystallite size of

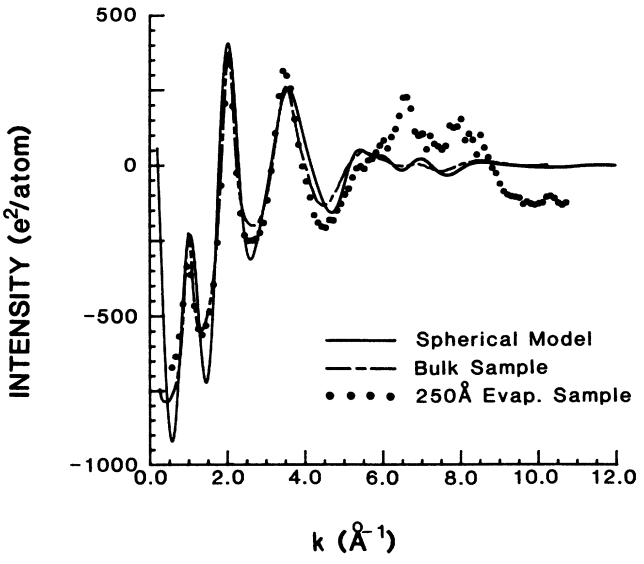

FIG. 3. A comparison of the spherical modeling results (solid) and the data from a bulk $GeSe_2$ sample (dashed) and from a 250-Å-thick evaporated $GeSe_2$ sample (dots).

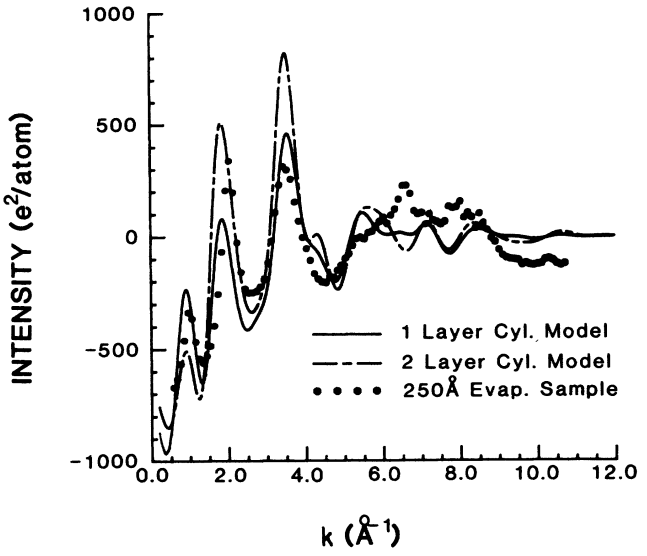

FIG. 4. A comparison of the one-layer cylindrical model (solid), the two-layer cylindrical model (dashed), and the data from a 250-Å-thick evaporated $GeSe_2$ sample (dots).

8–10 Å, with very little broadening of the distribution within this radius. We note that the lattice parameters of the crystal are $a=7.016$ Å, $b=16.796$ Å, and $c=11.831$ Å, where a is the distance along the $GeSe_2$ chains, $b/2$ is the separation between chains in the same layer, and $c/2$ is very close to the interlayer spacing. Thus, this microcrystallite model includes correlations within a chain and between chains as well as between layers.

Further analysis shows that the low-k peak in the SQC model comes from both interlayer and intralayer Ge-Ge correlations. Its origin is intrinsic to the nature of chemical ordering in the tetrahedral system, in that it arises from periodic density fluctuations. While the Se atoms also exhibit these fluctuations, there is a very large number of Se-Se second-nearest neighbors (within tetrahedra and between tetrahedra) which cancel positive contributions from other distances.

VI. CONCLUSIONS

Our results imply the amorphous material has short-range order similar to the crystalline phase since the SQC model is a good but not precise description of the a-$GeSe_2$ structure for first- and second-neighbor correlations (but not for longer-range order). The nature of the differences implies that, while there are features in the raft model which are consistent with the data, it is not an adequate description of the structure. In particular, we find no evidence of layers for films as thin as 250 Å, since the GIXS pattern did not change with sample thickness. Therefore, it appears that if there are layers, they have features which are different from the crystal and are not correlated in the same way.

The experimental results demonstrate the ability of the GIXS technique to isolate the signal of thin amorphous or highly disordered films on substrates. With the GIXS approach, it is currently possible to study amorphous thin films with the same x-ray techniques used to study bulk amorphous materials [x-ray scattering, DAS, extended x-ray-absorption fine structure (EXAFS) SAXS], though brighter x-ray sources will make these experiments easier. This ability opens up the possibility of studying classes of materials with x-ray techniques which could not be studied previously. Finally, we believe that the concept of studying the evolution of amorphous structure from two-dimensional to three-dimensional systems will prove to be a powerful technique in the study of intermediate-range order in amorphous systems.

ACKNOWLEDGMENTS

We would like to thank A. Bienenstock for very helpful discussions, and M. Marcus and J. DeNeufville for providing samples used in these experiments. A.F.C. received support from the Stanford Synchrotron Radiation Laboratory (SSRL), Stanford University, Stanford, California, for this work. This work was performed at SSRL, which is supported by the U.S. Department of Energy, Office of Basic Energy Sciences, and the National Institutes of Health, Bethesda, Maryland, Biotechnology Resource Program.

*Current address: Hewlett-Packard Laboratories, Palo Alto, CA 94304.

[1]P. Tronc, M. Bensoussan, A. Brenac, and C. Sebenne, Phys. Rev. B **8**, 5947 (1973).

[2]J. C. Phillips, J. Non-Cryst. Solids **43**, 37 (1981).

[3]P. Boolchand, J. Grothaus, W. J. Bresser, and P. Suranyi, Phys. Rev. B **25**, 2975 (1982).

[4]P. M. Bridenbaugh, G. P. Espinosa, J. E. Griffiths, J. C. Phillips, and J. R. Remeika, Phys. Rev. B **20**, 4140 (1979).

[5]K. Murase and T. Fukunaga, *Optical Effects in Amorphous Semiconductors,* in Proceedings of the International Topical Conference on Optical Effects in Amorphous Semiconductors, AIP Conf. Proc. No. 120, edited by P. C. Taylor and S. G. Bishop (AIP, New York, 1984), p. 449.

[6]J. E. Griffiths, G. P. Espinosa, J. P. Remeika, and J. C. Phillips, Solid State Commun. **40**, 1077 (1981); Phys. Rev. B **25**, 2971 (1982).

[7]O. Uemura, Y. Sagara, D. Muno, and T. Satow, J. Non-Cryst. Solids **30**, 155 (1978).

[8]K. F. Ludwig, Stanford Synchrotron Radiation Laboratory Report No. 86/06, 1986 (unpublished).

[9]W. C. Marra, P. H. Fuoss, and P. Eisenberger, Phys. Rev. Lett. **49**, 1169 (1982); P. Eisenberger and W. C. Marra, *ibid.* **46**, 1081 (1981).

[10]P. H. Fuoss, Ph.D. thesis, Stanford University, 1980; Stanford Synchrotron Radiation Laboratory Report No. 80/06, 1980 (unpublished).

[11]P. H. Fuoss, P. Eisenberger, W. K. Warburton, and A. Bienenstock, Phys. Rev. Lett. **46**, 1537 (1981).

[12]M. P. Taylor, Ph.D. thesis, Stanford University, 1978.